

1 **A Simple Framework for Likely Climate Projections Applied to Tropical Width**

2 **Daniel Baldassare<sup>1</sup>, Thomas Reichler<sup>1</sup>**

- 3 • <sup>1</sup>Department of Atmospheric Sciences, University of Utah, Salt Lake City, UT 84112,  
4 USA

5 Correspondence: Daniel Baldassare (daniel.baldassare@utah.edu)

6

7 **Abstract**

8 The increasing use of climate projections in adaptation necessitates a consistent method for  
9 producing estimates of likely future conditions from available climate model data. Many climate  
10 projections are produced using high emission scenarios and an evenly weighted ensemble of all  
11 available climate models despite substantial evidence that the continuously rising emissions in  
12 high emission scenarios are unrealistic, and that some models are more reliable than others. While  
13 high emission scenarios can be used to generate a more significant climate change signal and are  
14 often not intended to be interpreted as projections, a reader who is a non-expert on climate  
15 scenarios may not understand this nuance. As a result, unlikely climate projections could be  
16 inadvertently used to plan crucial adaptation efforts for future warming. Here, we present a simple  
17 and easy to use framework for creating projections of our likely future climate by combining  
18 existing methods. The framework involves three measures: selecting the most likely emission  
19 scenario, choosing the most reliable models, and debiasing against observational or reanalysis data.  
20 Each of these steps allows for a range of methods with varying complexity, precision, and utility.  
21 To demonstrate our framework and its components, we use the simplest applicable methods to  
22 estimate future changes in tropical width, a hydrologically important climate feature. Our  
23 projections show that the likely tropical expansion by the end of this century is roughly half of

24 some previously reported estimates, largely due to the selected emission scenario. This simple  
25 framework can be easily applied to other climate features, allowing for better estimates of likely  
26 future conditions.

27

28

29

30

31

32

33

34

35

36

37

38

39

40

41

42

43

44

45

46

47 **Introduction**

48         Adapting to our changing climate requires accurate information about the likely future.  
49 However, extracting estimates of probable future conditions from climate model simulations is  
50 challenging because the emissions scenarios and participating models of the Coupled Model  
51 Intercomparison Project (CMIP) differ so greatly. Simple variations in data processing methods  
52 such as model selection can produce a wide range of climate projections, complicating adaptation  
53 efforts. Recent estimates of future emissions and warming indicate that some simulations are more  
54 realistic than others, allowing for more precise estimates of probable future conditions. However,  
55 studies have often used implausibly high emission scenarios and included less-realistic models  
56 (Hausfather and Peters, 2020a), creating a situation where the prevalence of these simulations  
57 could cause improbable projections to be interpreted as our likely future. Here, we present a simple  
58 framework which uses probable estimates of future emissions, removes less realistic models, and  
59 debiases model outputs to create more realistic projections of the likely future climate.

60         In the last few years, substantial evidence has emerged that the high emission CMIP  
61 scenarios RCP 8.5 and SSP5-8.5 do not represent a plausible future (Hausfather and Peters, 2020b;  
62 Huard et al., 2022; Srikrishnan et al., 2022). Multiple recent reports suggest that global CO<sub>2</sub>  
63 emissions will peak before 2025 (Climate Analytics 2023, IEA 2023, BloombergNEF 2024), in  
64 disagreement with the continuously rising emissions in the high emission scenarios. This change  
65 in thought is further demonstrated by the recent interest by the ScenarioMIP working group in  
66 using a less intense high emission scenario than RCP 8.5 or SSP5-8.5 in CMIP7 due to these  
67 scenarios becoming increasingly unlikely (van Vuuren et al., 2023). While high emission scenarios  
68 should be considered as a low probability, high consequence potential future (Schwalm et al.,  
69 2020; Kemp et al., 2022), the implausibility of the current high emission scenarios limits their

70 utility for planning purposes. Additionally, more realistic scenarios such as SSP2-4.5 have been  
71 less frequently studied than these high emission scenarios, creating a relative scarcity of more  
72 probable future climate projections (Pielke and Ritchie, 2020; Burgess et al., 2022). Although  
73 SSP2-4.5 is less extreme than SSP5-8.5, it still represents a substantially warmer future, with  
74 severe societal and ecological impacts necessitating strong adaptation and mitigation (Cook et al.,  
75 2020; Spinoni et al., 2021).

76 High emission scenarios are often chosen in theoretical studies to create larger signal-to-  
77 noise ratios, or due to data availability. Notably, many studies are explicit in describing these  
78 scenarios as a high-emission future or worst-case scenario. However, due to the prevalence of  
79 studies which have used this scenario, a reader who is not an expert in climate scenarios may  
80 assume that these studies are projections of a probable future. In addition, it may be interpreted  
81 that the frustratingly slow progress on decarbonization suggests that the high emission scenario is  
82 likely. Regardless, because of the focus on high emission scenarios, the estimates of probable  
83 future conditions necessary for adaptation are underreported for many parts of the climate system.

84 In addition to focusing on implausible scenarios, many projections have used ensembles  
85 which include less reliable models. A sizable portion of CMIP6 models have climate sensitivities  
86 which are improbable, primarily due to being too large, decreasing the representativeness of both  
87 the ensemble spread and mean (Sherwood et al., 2020; Liang et al., 2020; Tierney et al., 2020;  
88 Hausfather et al., 2022). One easily calculated climate sensitivity metric, the transient climate  
89 response (TCR), measures the relationship between temperature increase and carbon dioxide  
90 increase once carbon dioxide concentration has doubled. The International Panel on Climate  
91 Change Sixth Assessment Report (IPCC-AR6) calculated TCR by combining multiple methods,  
92 resulting in the estimated likely ( $1\sigma$ ) range of 1.4-2.2 K (Arias et al., 2021), which we also use in

93 this study. Because climate models vary so greatly, as measured by TCR and other metrics, many  
94 techniques have been developed for creating weighted ensembles based on model skill (Brunner  
95 et al., 2020a). For example, by weighting models based on performance and independence,  
96 Brunner et al. (2020b) projected less intense warming from CMIP6 models. Here, we focus our  
97 model selection on TCR in an effort to present a simple version of this framework, though  
98 considering other metrics of model performance may also prove useful.

99         The final procedure in our framework is to debias the models. Biases in individual models  
100 and the ensemble mean have been well documented in CMIP6, with only modest improvements  
101 relative to CMIP5 (Kim et al., 2020). Because of this issue, a variety of methods for debiasing  
102 have been proposed, from simple mean subtraction to more advanced methods (Teutschbein and  
103 Seibert, 2012). In addition to discussion over the benefits of each method, the utility of debiasing  
104 has been debated for some applications (Laux et al., 2021), though some have argued that the  
105 negative effects of bias correction are not detectable (Maraun et al., 2017). To present a simple  
106 version of the debiasing without introducing large and potentially spurious changes to the tropical  
107 width projections, we focus on removing the minor circulation change biases associated with the  
108 present-day circulation, similar to those previously reported in Kidston and Gerber (2010),  
109 Simpson and Polvani (2016), Curtis et al. (2020), and Simpson et al. (2021).

110         We create projections of tropical width to showcase our proposed framework and the  
111 impact of each of its measures. Tropical width is a societally important feature of the climate  
112 system, as the poleward edge of the tropics is associated with sharp latitudinal gradients in  
113 precipitation (Lu et al., 2007; Schmidt and Grise, 2017). Over the satellite era (1979-present), the  
114 latitudinal width of the tropics has increased due to many factors including natural variability,  
115 global warming, and stratospheric ozone depletion (Grise et al., 2019; Waugh et al., 2015). While

116 temperature is projected to increase in the 21<sup>st</sup> century under all CMIP6 scenarios, stratospheric  
117 ozone depletion peaked at the end of the 20<sup>th</sup> century and is projected to decline in the 21<sup>st</sup> century  
118 (WMO, 2022), countering the increase in tropical extent associated with warming (Perlwitz, 2011).

119         Recent tropical width modeling studies either focused primarily on the high emission  
120 scenarios or included multiple scenarios with no emphasis on which projections are most probable.  
121 For example, Staten et al. (2018) and Grise and Davis (2020) only considered the high emission  
122 scenarios RCP 8.5 and SSP5-8.5 respectively. Tao et al. (2016), Allen and Ajoku (2016), and Xia  
123 et al. (2020) analyzed several scenarios, showing that tropical widening trends increase with  
124 emission intensity. Of these five studies, none considered model sensitivity, resulting in models  
125 with TCR outside of the likely range being included in the analyses. Using our simple framework,  
126 we attempt to project the most probable future tropical edge latitude and compare our results  
127 against those derived from methods such as those from Grise and Davis (2020). As we will show,  
128 our framework leads to a substantial reduction in estimated tropical expansion compared to these  
129 methods.

130

## 131 **Data and Methods**

132         We used CMIP6 (Eyring et al., 2016) zonal surface-wind and 2m air temperature data for  
133 the historical period 1850-2014 and for three forcing levels from 2015-2099: SSP1-2.6, SSP2-4.5,  
134 and SSP5-8.5. Zonal surface-wind and temperature data were acquired for all available CMIP6  
135 models (Table 1). We selected 28 models based on the availability of data for both variables across  
136 all three forcings. TCR values were acquired from Hausfather et al. (2022) and checked against  
137 Njisse et al. (2020). Of the 28 models, 1 has a TCR of less than 1.4 K, 19 have TCR values in the  
138 likely range of 1.4-2.2 K calculated in IPCC-AR6 (Arias et al., 2021), and 8 have TCR values

139 greater than 2.2 K. To provide observation-based estimates of the present-day tropical width, we  
140 used monthly averaged ERA5 (Hersbach et al., 2020) reanalysis data for zonal surface-wind from  
141 the satellite era (1979-2014). This period was chosen as a compromise between length and quality  
142 as there are fewer remote observations before 1979.

143 ERA5 is chosen as it is the successor to ERA-Interim, which is shown in Davis and Davis  
144 (2018) and Chemke and Polvani (2019) to be physically reasonable for phenomena associated with  
145 Hadley cell width and circulation strength. ERA5 is chosen over ERA-Interim due to the improved  
146 resolution and accuracy (Hersbach et al., 2020), and a recent study demonstrating that ERA5  
147 produces internally consistent estimates of Hadley cell width using the chosen metric (Baldassare  
148 et al., 2023).

149 Zonal surface-wind data from both ERA5 and CMIP6 were zonally and annually averaged  
150 and then used to compute the latitudes of the tropical edge over the two hemispheres using the  
151 zonal surface-wind zero crossing method in the software package PyTropD (Adam et al., 2018).  
152 PyTropD uses spline interpolation to determine the tropical edge latitude, decreasing the impact  
153 of resolution differences between models. The zonal surface-wind zero crossing method is chosen  
154 over other methods such as the meridional stream function due to the consistency in estimates from  
155 ERA5 (Baldassare et al., 2023), though similar results were obtained using the meridional stream  
156 function (not shown). Annual mean global averages of 2-meter temperature were computed from  
157 CMIP6.

158 For both ERA5 and CMIP6, uncertainties are calculated through bootstrapping, using  
159 10,000 samples with replacement. To focus on the likely changes to tropical width, we use the  $1\sigma$   
160 uncertainty range throughout, consistent with the likely range from IPCC-AR6 (Arias et al., 2021).  
161 For the final projections shown in Figure 6, the uncertainty range is calculated by summing the

162 bootstrapped uncertainties of the 30-year mean of the model projected tropical edge latitude,  
 163 present-day ERA5 tropical edge latitude, and the uncertainty of the ensemble mean.

164

165 Table 1: CMIP6 models used in this study with associated TCR values. Models with TCR below  
 166 likely range of 1.4-2.2 K are marked in green, while those with TCR values greater than this range  
 167 are in red.

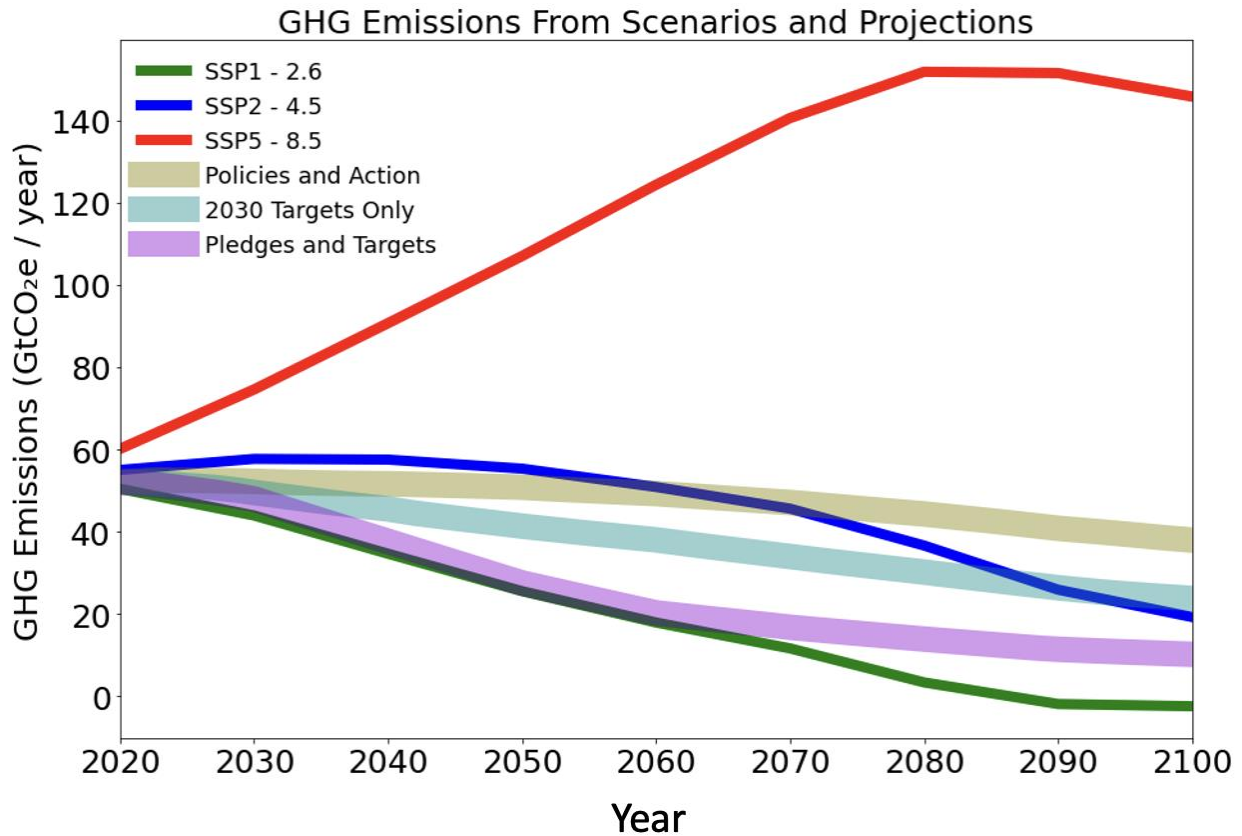
<b>Number</b>	<b>Model</b>	<b>TCR (K)</b>
<b>1</b>	<b>ACCESS-CM2</b>	<b>1.96</b>
<b>2</b>	<b>ACCESS-ESM1-5</b>	<b>1.97</b>
<b>3</b>	<b>AWI-CM-1-1-MR</b>	<b>2.03</b>
<b>4</b>	<b>BCC-CSM2-MR</b>	<b>1.55</b>
<b>5</b>	<b>CAMS-CSM1-0</b>	<b>1.73</b>
<b>6</b>	<b>CMCC-CM2-SR5</b>	<b>2.14</b>
<b>7</b>	<b>CMCC-ESM2</b>	<b>1.92</b>
<b>8</b>	<b>CNRM-CM6-1</b>	<b>2.22</b>
<b>9</b>	<b>CNRM-CM6-1-HR</b>	<b>2.46</b>
<b>10</b>	<b>CNRM-ESM2-1</b>	<b>1.83</b>
<b>11</b>	<b>CanESM5</b>	<b>2.71</b>
<b>12</b>	<b>CanESM5-CanOE</b>	<b>2.71</b>
<b>13</b>	<b>FGOALS-g3</b>	<b>1.50</b>
<b>14</b>	<b>GFDL-ESM4</b>	<b>1.63</b>
<b>15</b>	<b>HadGEM3-GC31-LL</b>	<b>2.49</b>
<b>16</b>	<b>IITM-ESM</b>	<b>1.66</b>
<b>17</b>	<b>INM-CM4-8</b>	<b>1.30</b>
<b>18</b>	<b>INM-CM5-0</b>	<b>1.41</b>
<b>19</b>	<b>IPSL-CM6A-LR</b>	<b>2.35</b>
<b>20</b>	<b>KACE-1-0-G</b>	<b>2.04</b>
<b>21</b>	<b>MCM-UA-1-0</b>	<b>1.90</b>
<b>22</b>	<b>MIROC-ES2L</b>	<b>1.49</b>
<b>23</b>	<b>MIROC6</b>	<b>1.55</b>
<b>24</b>	<b>MPI-ESM1-2-HR</b>	<b>1.64</b>
<b>25</b>	<b>MPI-ESM1-2-LR</b>	<b>1.82</b>
<b>26</b>	<b>MRI-ESM2-0</b>	<b>1.67</b>
<b>27</b>	<b>NESM3</b>	<b>2.72</b>
<b>28</b>	<b>UKESM1-0-LL</b>	<b>2.77</b>
	<b>Average for All Models</b>	<b>1.97</b>
	<b>Average for Likely TCR Models</b>	<b>1.76</b>

168



169 **Forcing Selection**

170 Choosing the most representative emission scenario is the most critical step in producing  
171 a likely climate projection. To select the forcing scenario, we suggest comparing the emissions  
172 from each scenario to trustworthy emissions projections and probabilistic emissions models. This  
173 flexible method allows for potential refinements in climate projections following the anticipated  
174 emergence of additional emission scenarios and improved emission projections. For this study, we  
175 begin by comparing the emissions from the three SSP scenarios to the “Policies and Action”, “2030  
176 Targets Only”, and “Pledges & Targets” projections from the Climate Action Tracker (Climate  
177 Action Tracker, 2022). These three projections represent 21<sup>st</sup> century emissions resulting from  
178 different assumptions in the implementation of national emission reduction pledges. All three  
179 projections most closely match SSP2-4.5 while also projecting emissions which are less than 1/3  
180 of SSP5-8.5 emissions by the end of the century (Figure 1). None of the projections match SSP1-  
181 2.6 as the negative emissions needed for this scenario do not exist in the Climate Action Tracker  
182 projections. Next, we consider recent studies comparing each scenario to probabilistic integrated  
183 assessment models (Srikrishnan et al., 2022; Huard et al., 2022), both of which indicate that SSP2-  
184 4.5 is the most likely scenario in the late 21<sup>st</sup> century. Following these comparisons, we conclude  
185 that SSP2-4.5 is currently the most likely scenario, while the frequently used SSP5-8.5 is very  
186 unlikely.



187

188

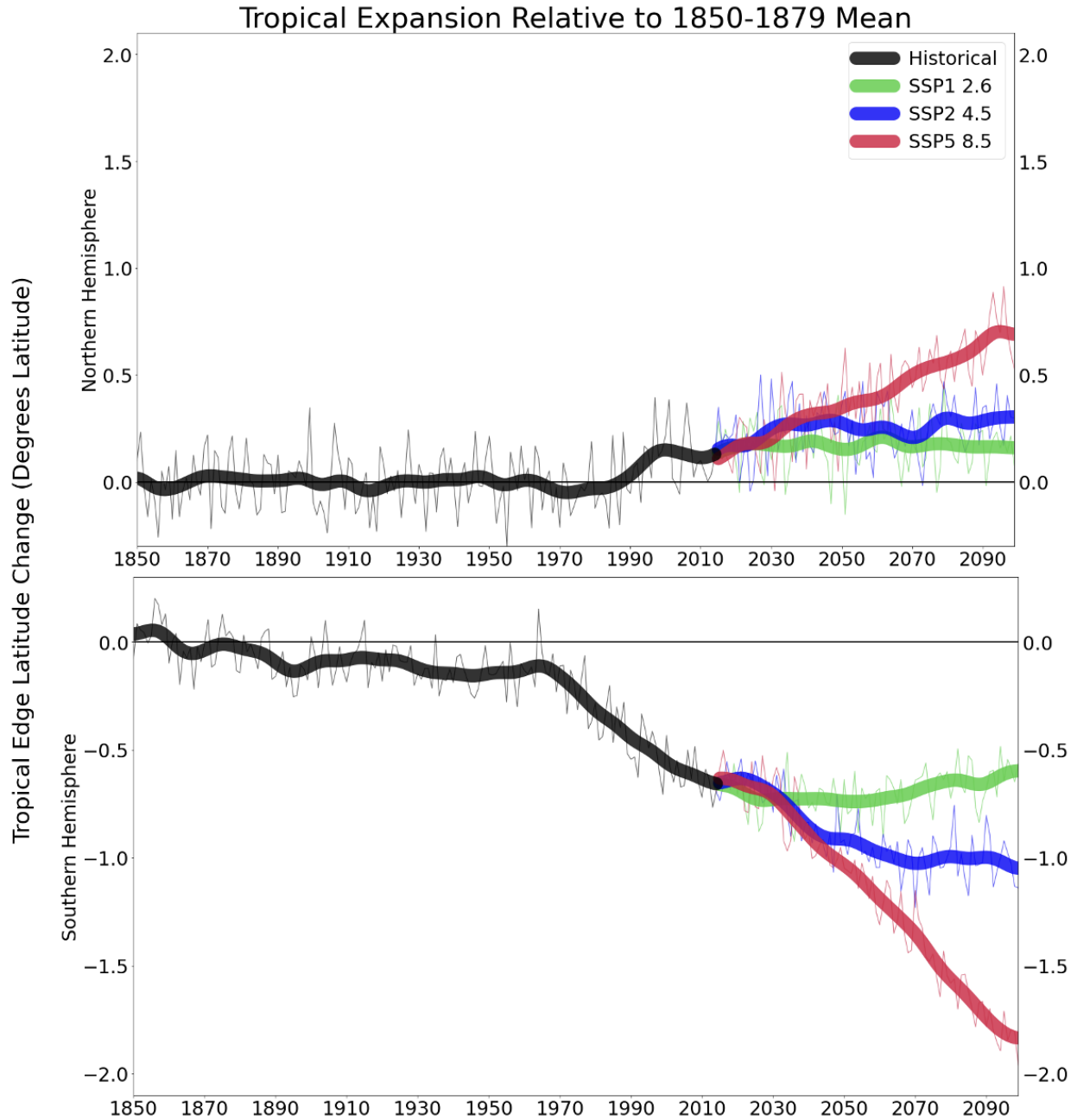
189 Figure 1: Greenhouse gas emissions from CO<sub>2</sub>, CH<sub>4</sub>, and N<sub>2</sub>O in gigaton of CO<sub>2</sub> equivalent per  
 190 year for three SSP scenarios and three Climate Action Tracker projections. Equivalent CO<sub>2</sub>  
 191 emissions are calculated by multiplying the CH<sub>4</sub> and N<sub>2</sub>O emissions by their respective global  
 192 warming potentials and adding these values to CO<sub>2</sub> emissions. Climate Action Tracker data is from  
 193 the Climate Action Tracker (Climate Action Tracker, 2022), and SSP scenario data is from Riahi  
 194 et al. (2017).

195

196 The importance of forcing selection is shown by the substantial differences in projected  
 197 tropical expansion between emission scenarios (Figure 2). The three scenarios shown are SSP1-  
 198 2.6, an improbable low-emission scenario which limits warming to around 1.5 °C; SSP2-4.5, the

199 most likely scenario with moderate emission reductions; and SSP5-8.5, an unlikely high-emission  
200 scenario with continuously rising emissions. In the Southern Hemisphere (SH), tropical expansion  
201 begins in the early 20<sup>th</sup> century and accelerates after 1960, coinciding with the start of ozone  
202 depletion (Polvani et al., 2011; Solomon et al., 2005), while the weaker Northern Hemisphere  
203 (NH) expansion only becomes noticeable after 1990. Because CMIP6 models project ozone  
204 recovery by the late 21<sup>st</sup> century (Revell et al., 2022), the larger SH expansion compared to the  
205 NH is unrelated to changes in ozone and indicates that the SH tropical width is more sensitive to  
206 the warming from increased greenhouse gases, in agreement with previous studies (Watt-Meyer  
207 et al., 2019). In addition, the greater sensitivity in the SH results in forcing differences which are  
208 larger than intermodel differences, in contrast to the NH where intermodel differences are greater  
209 (Fig. S1). As shown in Figure 2, by the end of the 21<sup>st</sup> century, the projected SH expansion under  
210 the low and high emission scenarios differs by a factor of three, and the expansion from SSP5-8.5  
211 is roughly twice that of SSP2-4.5.

212



213

214

215 Figure 2: Ensemble mean tropical edge latitude change relative to 1850-1879 for 28 CMIP6

216 models from three forcing scenarios. Thin lines represent the raw ensemble mean while thick lines

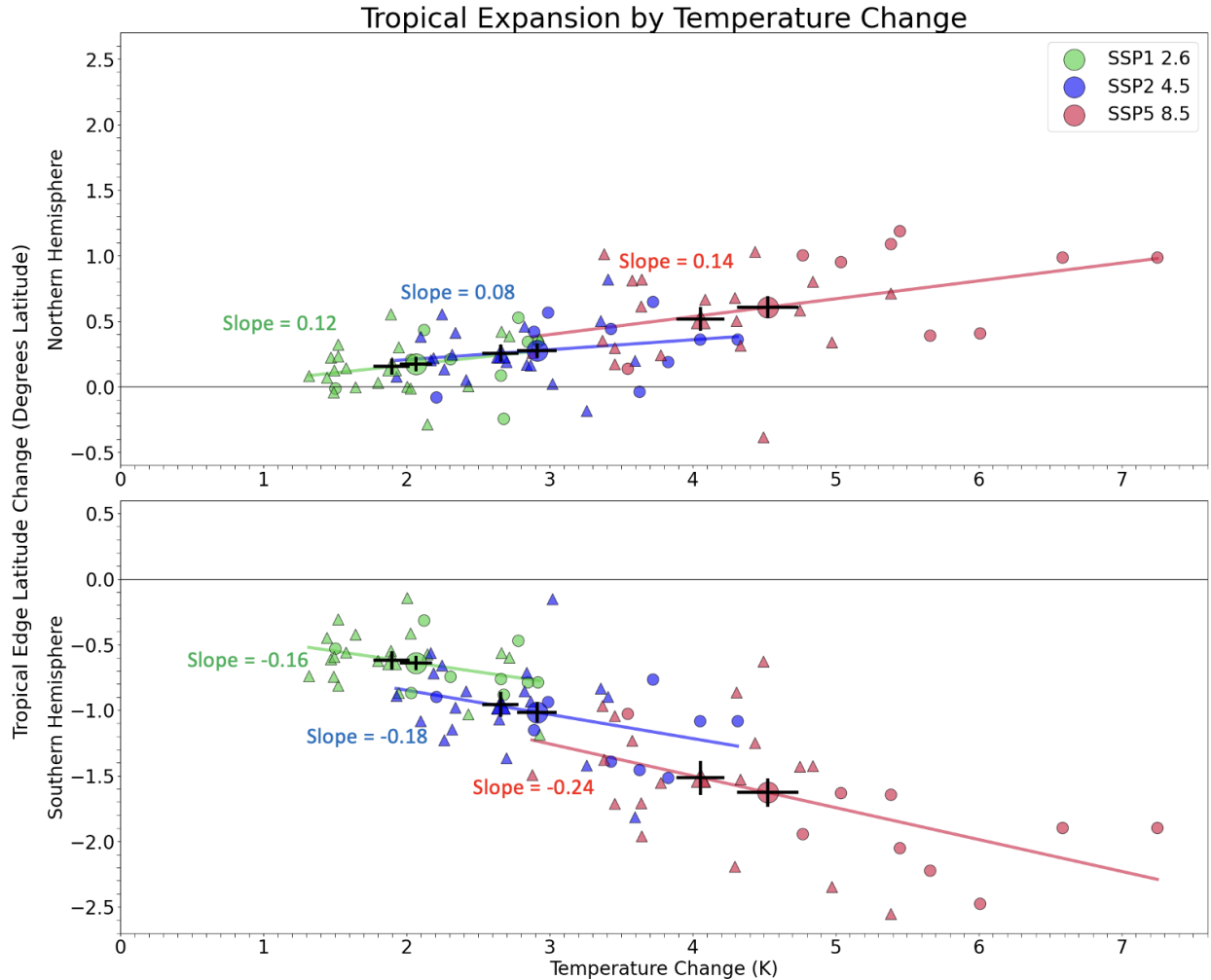
217 result from a Gaussian smoothing.

218

219 **Model Selection**

220 While selecting the most likely emission scenario SSP2-4.5 has a large impact on the  
221 tropical width projections, the full ensemble is still composed of models with implausible rates of  
222 future warming. We attempt to correct this issue by focusing on models with reasonable TCR  
223 values, discarding models outside of the likely climate sensitivity range of 1.4-2.2 K from IPCC-  
224 AR6 (Arias et al., 2021). Because more CMIP6 models have high TCR than low TCR values, our  
225 moderate ensemble has an average TCR of 1.76 K compared to the full ensemble average of 1.97  
226 K (Table 1).

227 For SSP2-4.5, the moderate TCR ensemble projects less warming and less tropical  
228 expansion than the full ensemble as shown by the difference between the ensemble averages  
229 (Figure 3). There is an approximately linear relationship between warming and tropical expansion,  
230 with a greater slope in the SH and for higher forcing simulations. Although the slopes of the  
231 regression lines for all three scenarios are positive, they are significantly different from zero at the  
232 two-sided 95% confidence level only for the high forcing simulations in both hemispheres. For all  
233 scenarios in both hemispheres, the larger temperature increase projected by the full ensemble  
234 results in more expansion than the moderate TCR ensemble. Because of the greater sensitivity, the  
235 TCR filtering is more impactful in the SH, similar to the forcing selection shown previously.



236

237

238 Figure 3: Changes in tropical edge and temperature from 1850-1879 to 2070-2099. Models with  
 239 TCR values between 1.4 and 2.2 K are denoted by triangles, and models with TCR outside of this  
 240 likely range are marked as circles. Large symbols denote ensemble means with their 1σ range,  
 241 with the large circle representing the ensemble mean of all models, and the large triangle  
 242 representing the mean of moderate TCR models. For each forcing level, a linear best fit from all  
 243 28 models is displayed in the corresponding color.

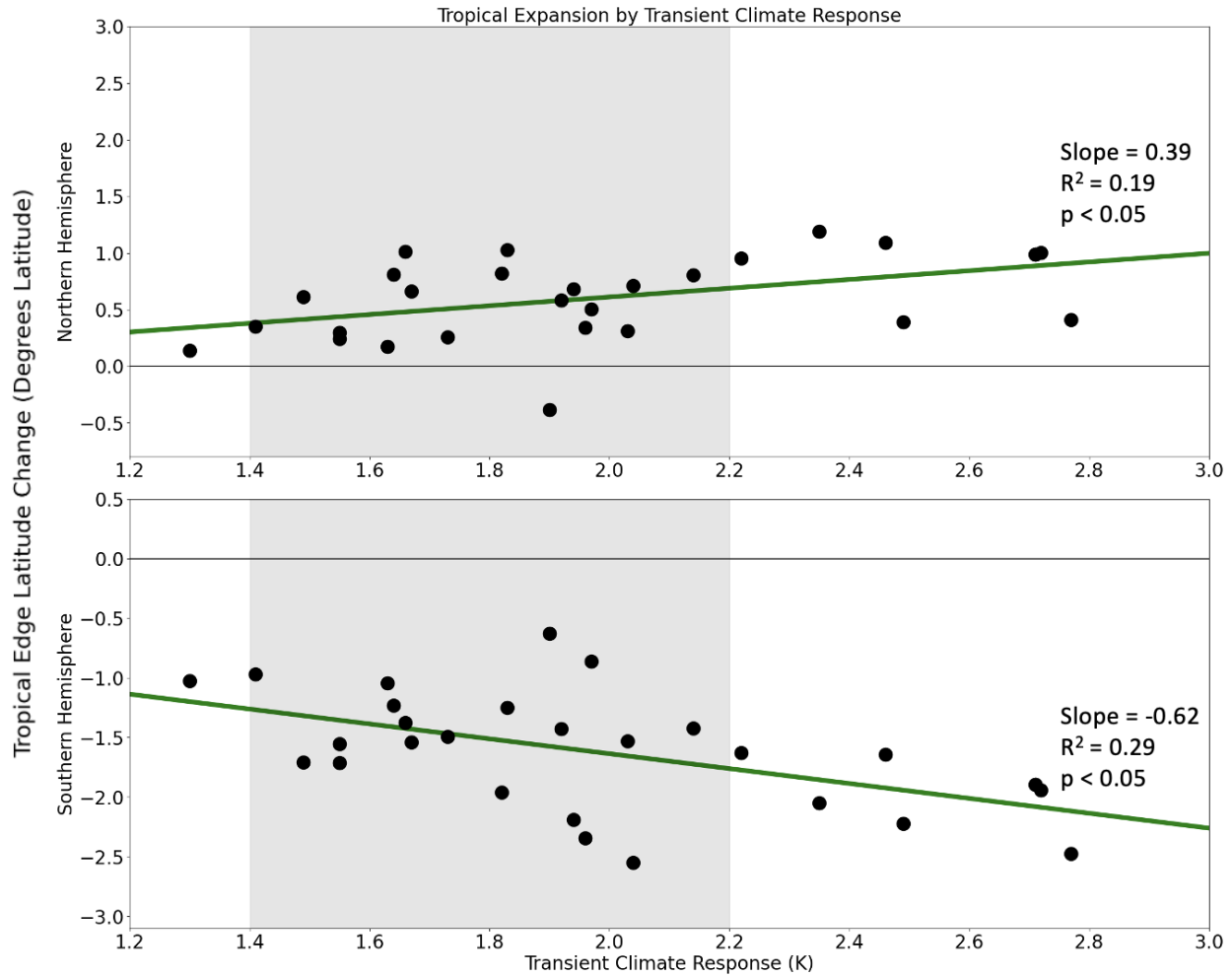
244

245 Previous studies found an insignificant relationship in the NH between tropical widening  
246 and equilibrium climate sensitivity, which measures temperature change once climate has reached  
247 equilibrium following a pulse of carbon dioxide (Grise and Polvani, 2014; Grise and Polvani,  
248 2016; De et al., 2021). However, we find that TCR is significantly correlated with tropical  
249 widening in both hemispheres, requiring the removal of overly sensitive models for realistic  
250 tropical width projections (Figure 4). The disagreement between our study and previous studies  
251 could be the result of different models or metrics, but may also be due to the fact that by 2100 the  
252 scenario simulations are not yet in equilibrium, causing TCR to be a better predictor of the  
253 projected 21<sup>st</sup> century warming and widening than equilibrium climate sensitivity.

254

255

256



257

258

259 Figure 4: Projected tropical edge latitude change (2070-2099 – 1850-1869) by transient climate  
 260 response for all CMIP6 models using SSP5-8.5. The shaded gray region denotes the likely TCR  
 261 range of 1.4-2.2 K according to IPCC-AR6 (Arias et al., 2021).

262

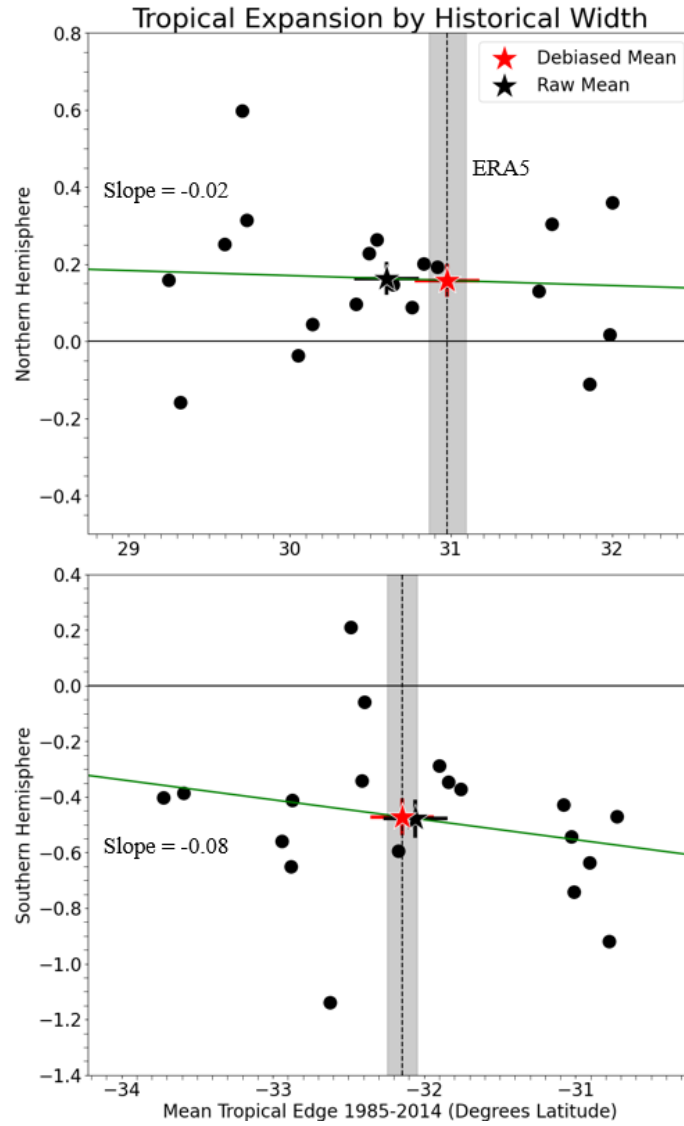
### 263 **Debiasing Model Outputs**

264 Now that we have chosen the most likely emission scenario and constructed an ensemble  
 265 of the most reasonable models, the final measure is to debias the models. Depending on the feature  
 266 of interest, debiasing may be necessary due to limitations in climate simulations (Laux et al., 2021).



267 For example, both individual models and ensembles have been shown to inaccurately represent  
268 satellite era precipitation in the tropics (Kim et al., 2020). These issues may become especially  
269 pronounced when focusing on a subset of precipitation or a more specific region or time period,  
270 an example being the large 95<sup>th</sup> percentile precipitation biases in October through December in  
271 East Africa shown in Ayugi et al. (2021). As here we are focusing on zonally averaged features of  
272 the annual mean Hadley cell, a climate feature which is generally well simulated (Chemke and  
273 Polvani, 2019), debiasing may not be as beneficial and could introduce spurious changes as  
274 observed from other debiasing methods (Cannon et al., 2015). To demonstrate this step in the  
275 framework without introducing large and questionable changes to the projections, we choose to  
276 perform a relatively simple debiasing, focusing on a minor and statistically insignificant tendency  
277 for models with equatorward biased jets tend to exhibit more widening than other models (Kidston  
278 and Gerber, 2010; Simpson and Polvani, 2016; Curtis et al., 2020; Simpson et al., 2021). To  
279 analyze whether present-day biases in the latitude of the Hadley cell edge exhibit a similar  
280 relationship in the chosen CMIP6 models, we calculate the corresponding statistics for each model  
281 (Figure 5). Similar to previous studies (Kidston and Gerber, 2010; Simpson and Polvani, 2016;  
282 Curtis et al., 2020; Simpson et al., 2021), we find that the models with equatorward biased present-  
283 day tropical width project more future widening in both hemispheres. While Figure 5 shows the  
284 results for 2070-2099, this feature is present throughout the 21st century, though it is not  
285 statistically significant. Because the ensemble mean present-day tropical edge is biased  
286 equatorwards relative to ERA5 in both hemispheres, roughly 0.3 degrees in the NH and 0.1 degrees  
287 in the SH, the tendency for equatorward biased models to project more expansion may result in an  
288 overestimation of future expansion.

289



290

291

292 Figure 5: Tropical expansion between 1985-2014 and 2070-2099 by 1985-2014 tropical edge  
 293 latitude for moderate TCR models using SSP2-4.5. The stars denote the raw (black) and debiased  
 294 (red) ensemble means, with the 1σ range shown. The vertical dashed line marks the mean tropical  
 295 edge in ERA5 from 1985-2014 with the gray shaded region depicting the 1σ range calculated from  
 296 bootstrapping. The green line is a linear best fit of all models prior to debiasing.  $R^2$  is nearly zero  
 297 in both hemispheres.

298

299 To debias the projections, we remove this tendency from the models by the following  
 300 process, which is performed in each year  $j$  and repeated for both hemispheres as demonstrated in  
 301 Fig. S2. First, the present-day (1985-2014) tropical edge for each model  $\phi_i$  and for ERA5  $\phi_{ERA5}$  is  
 302 calculated, as well as the future tropical edge in each model, using 30-year mean data centered on  
 303 the year of interest  $j$ . For each model  $i$  in each year  $j$ , the present-day tropical edge  $\phi_i$  is subtracted  
 304 from the future tropical edge, resulting in the change of tropical edge  $\Delta\phi_{i,j}$ . A linear best fit is  
 305 calculated between the tropical edge changes and present-day tropical edges of all models in each  
 306 year  $j$ , producing the intercept  $a_j$  and slope  $b_j$ . Next, from the linear best fit, each model's estimated  
 307 expansion  $\Delta\hat{\phi}_{i,j}$  is

$$308 \quad (1) \quad \Delta\hat{\phi}_{i,j} = a_j + b_j\phi_i ,$$

309 and the residual  $\varepsilon_{i,j}$ , which is the difference between the estimated and the actual expansion, is

$$310 \quad (2) \quad \varepsilon_{i,j} = \Delta\phi_{i,j} - \Delta\hat{\phi}_{i,j} .$$

311 Finally, the debiased expansion  $\Delta\tilde{\phi}_{i,j}$  is given by the sum of the expansion projected by the best  
 312 fit line at the ERA5 present-day edge and the residual

$$313 \quad (3) \quad \Delta\tilde{\phi}_{i,j} = a_j + b_j\phi_{ERA5} + \varepsilon_{i,j} = \Delta\phi_{i,j} + b_j(\phi_{ERA5} - \phi_i) .$$

314 This results in small reductions in projected expansion, which are not statistically significant in  
 315 either hemisphere, and are larger in later years and in the NH. While in this example the debiasing  
 316 has minor impacts, for climate features with large known biases such as extreme precipitation,  
 317 debiasing may be useful for providing more realistic projections (Xu et al., 2021).

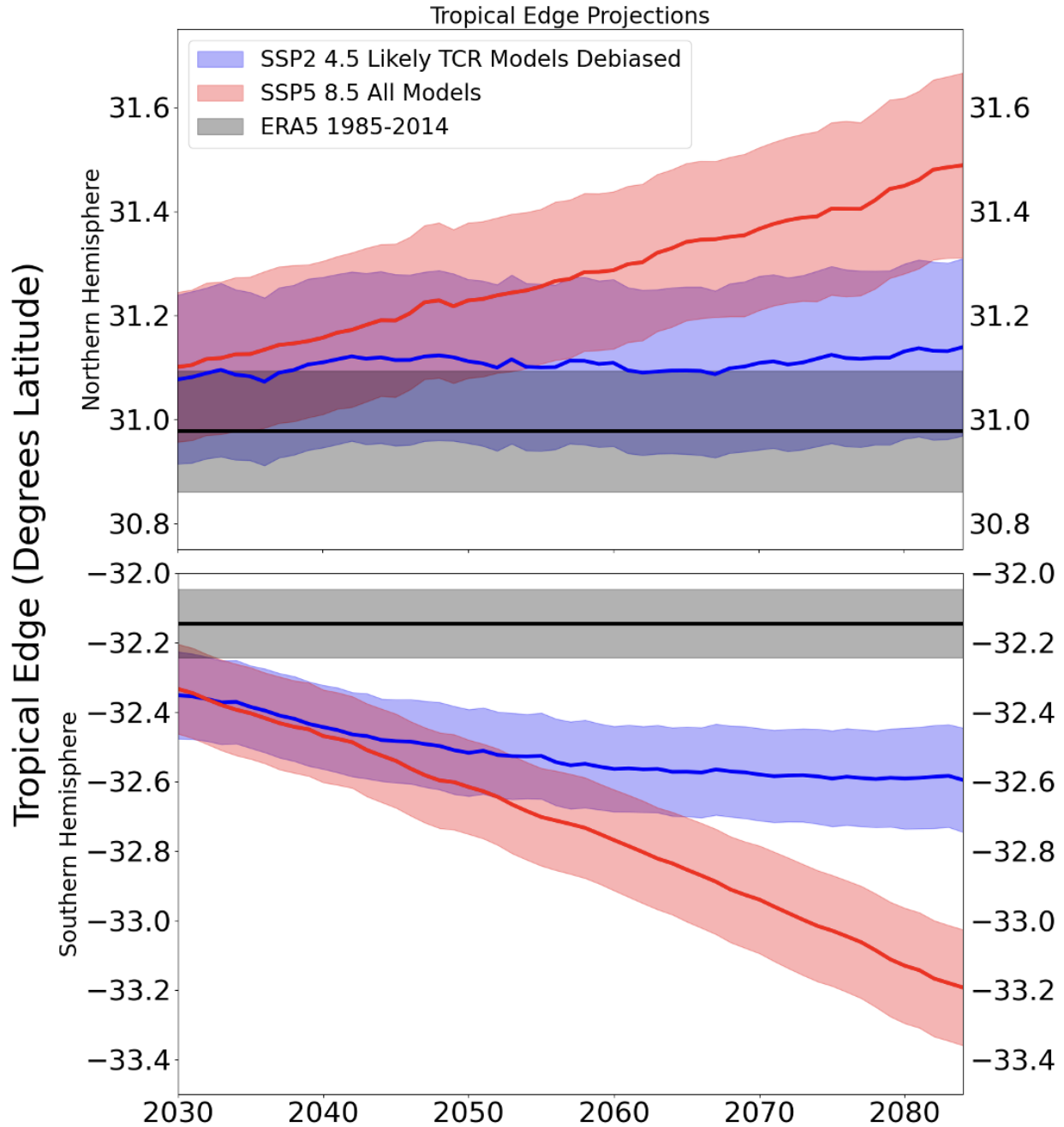
318

### 319 **Likely Tropical Width Projections**

320 In Figure 6, we compare the projections from our simple framework (blue) to those from a  
 321 more “typical” methodology such as Grise and Davis (2020) (red), which uses an ensemble of all

322 CMIP6 models with SSP5-8.5 as the forcing scenario. Compared to this methodology, our  
323 framework projects roughly half of the tropical expansion. The decrease is primarily the result of  
324 using the moderate emission scenario, though the TCR selection results in a further reduction in  
325 expansion. Our framework (Figure 6, blue) projects a 21<sup>st</sup> century tropical widening of 0.1 degrees  
326 in the NH, which is within the likely range of the late 20<sup>th</sup> century as measured by the 1 $\sigma$  range of  
327 the ERA5 mean (1985-2014). In contrast, the projected 21<sup>st</sup> century SH widening of 0.5 degrees  
328 is significant, further demonstrating the hemispheric differences in sensitivity. These results  
329 strongly differ from the projections of expansion from “typical” methods (Figure 6, red), which  
330 are significant at the 1 $\sigma$  level in both hemispheres. The “typical” methods (Figure 6, red) estimate  
331 roughly 0.5 degrees of expansion in the NH and 1.1 degrees in the SH. The differences between  
332 our framework and the previous approaches are larger in the SH due to the greater sensitivity,  
333 although by the end of the 21<sup>st</sup> century the difference is also significant in the NH. Following our  
334 methodology, the best estimate for the absolute position of the tropical edge at the end of the 21<sup>st</sup>  
335 century is 31.1 degrees in the NH and 32.6 degrees in the SH.

336



337

338

339 Figure 6: Tropical edge latitude following “typical” approaches (red) and the proposed framework  
 340 (blue). The value presented for each year is the 30-year mean centered on the year of interest. The  
 341 “typical” approach described here uses the mean of all CMIP6 models under SSP5-8.5. Our  
 342 framework includes only the models with moderate TCR values, uses SSP2-4.5 as forcing, and

343 debiases the relationship between present-day tropical edge bias and future expansion. In addition,  
344 for both methods we subtract the ERA5 present-day mean to remove mean biases. The thick areas  
345 in each color represent the  $1\sigma$  range from bootstrapping.

346

## 347 **Summary and Discussion**

348       Following our methodology, the likely end of century NH expansion relative to present is  
349 about 0.1 degrees while the SH expansion is roughly 0.5 degrees, both of which are considerably  
350 smaller than the estimates from methods used in some previous studies, for example Grise and  
351 Davis (2020) (Figure 6). Each measure of our proposed framework has distinct impacts on the  
352 projected tropical expansion. Focusing on the more likely moderate emission scenario roughly  
353 halves the expansion in both hemispheres. Excluding models with TCR values outside of a likely  
354 range decreases projected warming, causing a further reduction in expansion of roughly 0.1  
355 degrees globally, primarily due to reduced expansion in the Southern Hemisphere. The removal of  
356 model biases similar to Kidston and Gerber (2010), Simpson and Polvani (2016), Curtis et al.  
357 (2020), and Simpson et al. (2021) further decreases projected expansion in both hemispheres.

358       The framework we have described creates probable projections of future climate using  
359 available climate model data. The measures in this framework are adaptable for different  
360 applications and can be modified as better information or methods become available. The emission  
361 scenario selection will likely change due to revised estimates of future emissions and the creation  
362 of new scenarios. Additionally, the emission selection could be improved through the  
363 consideration of other relevant factors such as aerosols, which have spatially heterogenous impacts  
364 and may be especially impactful for certain regions (Persad et al., 2023) or climate features (Zhao  
365 et al., 2020). The model selection could be refined by considering multiple measures of skill based

366 on historical observations or theoretical arguments, or by using a more sophisticated weighting  
367 method. For some climate features the debiasing step could be ignored, while for other features,  
368 debiasing could be modified by utilizing methods tailored to the system of interest. As it stands,  
369 the simple methods presented here produce improved climate projections with minimal effort.

370

371

372

373

374

375

376

377

378

379

380

381

382

383

384

385

386

387

388

389 **Bibliography**

- 390 Adam, O., Grise, K. M., Staten, P., Simpson, I. R., Davis, S. M., Davis, N. A., Waugh, D. W.,  
391 Birner, T. and Ming, A.: The TROPD software package (V1): Standardized methods for  
392 calculating tropical-width diagnostics, *Geoscientific Model Development*, 11(10), 4339–  
393 4357, doi:10.5194/gmd-11-4339-2018, 2018.
- 394 Allen, R. J. and Ajoku, O.: Future aerosol reductions and widening of the northern tropical belt,  
395 *Journal of Geophysical Research: Atmospheres*, 121, 6765–6786,  
396 <https://doi.org/10.1002/2016JD024803>, 2016.
- 397 Arias, P.A., N. Bellouin, E. Coppola, R.G. Jones, G. Krinner, J. Marotzke, V. Naik, M.D.  
398 Palmer, G.-K. Plattner, J. Rogelj, M. Rojas, J. Sillmann, T. Storelvmo, P.W. Thorne, B.  
399 Trewin, K. Achuta Rao, B. Adhikary, R.P. Allan, K. Armour, G. Bala, R. Barimalala, S.  
400 Berger, J.G. Canadell, C. Cassou, A. Cherchi, W. Collins, W.D. Collins, S.L. Connors, S.  
401 Corti, F. Cruz, F.J. Dentener, C. Dereczynski, A. Di Luca, A. Diongue Niang, F.J. Doblus-  
402 Reyes, A. Dosio, H. Douville, F. Engelbrecht, V. Eyring, E. Fischer, P. Forster, B. Fox-  
403 Kemper, J.S. Fuglestedt, J.C. Fyfe, N.P. Gillett, L. Goldfarb, I. Gorodetskaya, J.M.  
404 Gutierrez, R. Hamdi, E. Hawkins, H.T. Hewitt, P. Hope, A.S. Islam, C. Jones, D.S.  
405 Kaufman, R.E. Kopp, Y. Kosaka, J. Kossin, S. Krakovska, J.-Y. Lee, J. Li, T. Mauritsen,  
406 T.K. Maycock, M. Meinshausen, S.-K. Min, P.M.S. Monteiro, T. Ngo-Duc, F. Otto, I.  
407 Pinto, A. Pirani, K. Raghavan, R. Ranasinghe, A.C. Ruane, L. Ruiz, J.-B. Sallée, B.H.  
408 Samset, S. Sathyendranath, S.I. Seneviratne, A.A. Sörensson, S. Szopa, I. Takayabu, A.-M.  
409 Tréguier, B. van den Hurk, R. Vautard, K. von Schuckmann, S. Zaehle, X. Zhang, and K.  
410 Zickfeld, 2021: Technical Summary. In *Climate Change 2021: The Physical Science Basis*.  
411 Contribution of Working Group I to the Sixth Assessment Report of the Intergovernmental  
412 Panel on Climate Change [Masson-Delmotte, V., P. Zhai, A. Pirani, S.L. Connors, C. Péan,  
413 S. Berger, N. Caud, Y. Chen, L. Goldfarb, M.I. Gomis, M. Huang, K. Leitzell, E. Lonnoy,  
414 J.B.R. Matthews, T.K. Maycock, T. Waterfield, O. Yelekçi, R. Yu, and B. Zhou (eds.)].  
415 Cambridge University Press, Cambridge, United Kingdom and New York, NY, USA, pp.  
416 33–144. doi:10.1017/9781009157896.002.
- 417 Ayugi, B., Zhihong, J., Zhu, H., Ngoma, H., Babaousmail, H., Rizwan, K., and Dike, V.:  
418 Comparison of CMIP6 and CMIP5 models in simulating mean and extreme precipitation  
419 over East Africa, *International Journal of Climatology*, 41, 6474–6496,  
420 <https://doi.org/10.1002/joc.7207>, 2021.
- 421 Baldassare, D., Reichler, T., Plink-Björklund, P. and Slawson, J.: Large uncertainty in observed  
422 estimates of tropical width from the meridional stream function, *Weather and Climate*  
423 *Dynamics*, 4(2), 531–541, doi:10.5194/wcd-4-531-2023, 2023.
- 424 BloombergNEF: *New Energy Outlook 2024*. 2024.
- 425 Brunner, L., McSweeney, C., Ballinger, A. P., Befort, D. J., Benassi, M., Booth, B., Coppola, E.,  
426 de Vries, H., Harris, G., Hegerl, G. C., Knutti, R., Lenderink, G., Lowe, J., Nogherotto, R.,



427 O'Reilly, C., Qasmi, S., Ribes, A., Stocchi, P. and Undorf, S.: Comparing methods to  
428 constrain future European climate projections using a consistent framework, *Journal of*  
429 *Climate*, 33(20), 8671–8692, doi:10.1175/jcli-d-19-0953.1, 2020.

430 Brunner, L., Pendergrass, A. G., Lehner, F., Merrifield, A. L., Lorenz, R. and Knutti, R.:  
431 Reduced global warming from CMIP6 projections when weighting models by performance  
432 and Independence, *Earth System Dynamics*, 11(4), 995–1012, doi:10.5194/esd-11-995-  
433 2020, 2020.

434 Burgess, M. G., Pielke, R. and Ritchie, J.: Catastrophic climate risks should be neither  
435 understated nor overstated, *Proceedings of the National Academy of Sciences*, 119(42),  
436 doi:10.1073/pnas.2214347119, 2022.

437 Cannon, A. J., Sobie, S. R., and Murdock, T. Q.: Bias Correction of GCM Precipitation by  
438 Quantile Mapping: How Well Do Methods Preserve Changes in Quantiles and Extremes?,  
439 *Journal of Climate*, 28, 6938–6959, <https://doi.org/10.1175/jcli-d-14-00754.1>, 2015.

440 Chemke, R. and Polvani, L. M.: Opposite tropical circulation trends in climate models and in  
441 reanalyses, *Nature Geoscience*, 12, 528–532, <https://doi.org/10.1038/s41561-019-0383-x>,  
442 2019.

443 Climate Action Tracker (2022). The CAT Thermometer. November 2022. Available at:  
444 <https://climateactiontracker.org/global/cat-thermometer/> Copyright © 2022 by Climate  
445 Analytics and NewClimate Institute. All rights reserved

446 Climate Analytics (2023). When will global emissions peak?

447 Cook, B. I., Mankin, J. S., Marvel, K., Williams, A. P., Smerdon, J. E. and Anchukaitis, K. J.:  
448 Twenty-first century drought projections in the CMIP6 forcing scenarios, *Earth's Future*,  
449 8(6), doi:10.1029/2019ef001461, 2020.

450 Curtis, P. E., Ceppi, P., and Zappa, G.: Role of the mean state for the Southern Hemispheric jet  
451 stream response to CO2 forcing in CMIP6 models, *Environmental Research Letters*, 15,  
452 064011, <https://doi.org/10.1088/1748-9326/ab8331>, 2020.

453 Davis, N. A. and Davis, S. M.: Reconciling Hadley Cell Expansion Trend Estimates in  
454 Reanalyses, *Geophysical Research Letters*, 45, <https://doi.org/10.1029/2018gl079593>,  
455 2018.

456 De, B., Tselioudis, G. and Polvani, L. M.: Improved representation of atmospheric dynamics in  
457 CMIP6 models removes climate sensitivity dependence on Hadley cell climatological  
458 extent, *Atmospheric Science Letters*, 23(3), doi:10.1002/asl.1073, 2021.

459 Eyring, V., S. Bony, G. A. Meehl, C. A. Senior, B. Stevens, R. J. Stouffer, and K. E. Taylor,  
460 2016: Overview of the Coupled Model Intercomparison Project Phase 6 (CMIP6)

461 experimental design and organization. *Geosci. Model Dev.*, **9**, 1937–1958,  
462 <https://doi.org/10.5194/gmd-9-1937-2016>.

463 Grise, K. M. and Davis, S. M.: Hadley cell expansion in CMIP6 models, *Atmospheric Chemistry*  
464 *and Physics*, 20(9), 5249–5268, doi:10.5194/acp-20-5249-2020, 2020.

465 Grise, K. M., Davis, S. M., Simpson, I. R., Waugh, D. W., Fu, Q., Allen, R. J., Rosenlof, K. H.,  
466 Ummenhofer, C. C., Karauskas, K. B., Maycock, A. C., Quan, X.-W., Birner, T. and  
467 Staten, P. W.: Recent tropical expansion: Natural variability or forced response?, *Journal*  
468 *of Climate*, 32(5), 1551–1571, doi:10.1175/jcli-d-18-0444.1, 2019.

469 Grise, K. M. and Polvani, L. M.: The response of Midlatitude Jets to increased CO<sub>2</sub>:  
470 Distinguishing the roles of sea surface temperature and direct radiative forcing,  
471 *Geophysical Research Letters*, 41(19), 6863–6871, doi:10.1002/2014gl061638, 2014.

472 Grise, K. M. and Polvani, L. M.: Is climate sensitivity related to dynamical sensitivity?, *Journal*  
473 *of Geophysical Research: Atmospheres*, 121(10), 5159–5176, doi:10.1002/2015jd024687,  
474 2016.

475 Hausfather, Z. and Peters, G. P.: Emissions – the ‘business as usual’ story is misleading, *Nature*,  
476 577(7792), 618–620, doi:10.1038/d41586-020-00177-3, 2020.

477 Hausfather, Z. and Peters, G. P.: RCP8.5 is a problematic scenario for near-term emissions,  
478 *Proceedings of the National Academy of Sciences*, 117(45), 27791–27792,  
479 doi:10.1073/pnas.2017124117, 2020.

480 Hausfather, Z., Marvel, K., Schmidt, G. A., Nielsen-Gammon, J. W. and Zelinka, M.: Climate  
481 simulations: Recognize the ‘Hot Model’ problem, *Nature*, 605(7908), 26–29,  
482 doi:10.1038/d41586-022-01192-2, 2022.

483 Hersbach, H., Bell, B., Berrisford, P., Hirahara, S., Horányi, A., Muñoz-Sabater, J., Nicolas, J.,  
484 Peubey, C., Radu, R., Schepers, D., Simmons, A., Soci, C., Abdalla, S., Abellan, X.,  
485 Balsamo, G., Bechtold, P., Biavati, G., Bidlot, J., Bonavita, M., Chiara, G., Dahlgren, P.,  
486 Dee, D., Diamantakis, M., Dragani, R., Flemming, J., Forbes, R., Fuentes, M., Geer, A.,  
487 Haimberger, L., Healy, S., Hogan, R. J., Hólm, E., Janisková, M., Keeley, S., Laloyaux, P.,  
488 Lopez, P., Lupu, C., Radnoti, G., Rosnay, P., Rozum, I., Vamborg, F., Villaume, S. and  
489 Thépaut, J. N.: The ERA5 global reanalysis, *Quarterly Journal of the Royal Meteorological*  
490 *Society*, 146(730), 1999–2049, doi:10.1002/qj.3803, 2020 (data available at:  
491 <https://cds.climate.copernicus.eu>, last access: 1 December 2023).

492 Huard, D., Fyke, J., Capellán-Pérez, I., Matthews, H. D. and Partanen, A. I.: Estimating the  
493 likelihood of GHG concentration scenarios from Probabilistic Integrated Assessment  
494 Model Simulations, *Earth's Future*, 10(10), doi:10.1029/2022ef002715, 2022.

495 IEA: World Energy Outlook 2023, <https://www.iea.org/reports/world-energy-outlook-2023>,  
496 2023.

497 Kemp, L., Xu, C., Depledge, J., Ebi, K. L., Gibbins, G., Kohler, T. A., Rockström, J., Scheffer,  
498 M., Schellnhuber, H. J., Steffen, W. and Lenton, T. M.: Climate endgame: Exploring  
499 catastrophic climate change scenarios, *Proceedings of the National Academy of Sciences*,  
500 119(34), doi:10.1073/pnas.2108146119, 2022.

501 Kidston, J. and Gerber, E. P.: Intermodel variability of the poleward shift of the austral jet stream  
502 in the CMIP3 integrations linked to biases in 20th century climatology, *Geophysical*  
503 *Research Letters*, 37(9), doi:10.1029/2010gl042873, 2010.

504 Kim, Y.-H., Min, S.-K., Zhang, X., Sillmann, J. and Sandstad, M.: Evaluation of the CMIP6  
505 multi-model ensemble for climate extreme indices, *Weather and Climate Extremes*, 29,  
506 100269, doi:10.1016/j.wace.2020.100269, 2020.

507 Knutti, R., Rugenstein, M. A. and Hegerl, G. C.: Beyond equilibrium climate sensitivity, *Nature*  
508 *Geoscience*, 10(10), 727–736, doi:10.1038/ngeo3017, 2017.

509 Laux, P., Rötter, R. P., Webber, H., Dieng, D., Rahimi, J., Wei, J., Faye, B., Srivastava, A. K.,  
510 Bliefernicht, J., Adeyeri, O., Arnault, J. and Kunstmann, H.: To bias correct or not to bias  
511 correct? an agricultural impact modelers' perspective on Regional Climate Model Data,  
512 *Agricultural and Forest Meteorology*, 304-305, 108406,  
513 doi:10.1016/j.agrformet.2021.108406, 2021.

514 Liang, Y., Gillett, N. P. and Monahan, A. H.: Climate model projections of 21st century global  
515 warming constrained using the observed warming trend, *Geophysical Research Letters*,  
516 47(12), doi:10.1029/2019gl086757, 2020.

517 Lu, J., Vecchi, G. A. and Reichler, T.: Expansion of the Hadley cell under Global Warming,  
518 *Geophysical Research Letters*, 34(6), doi:10.1029/2006gl028443, 2007.

519 Lucas, C., & Nguyen, H. (2015). Regional characteristics of tropical expansion and the role of  
520 climate variability. *Journal of Geophysical Research: Atmospheres*, 120(14), 6809–6824.  
521 <https://doi.org/10.1002/2015jd023130>

522 Maraun, D., Shepherd, T. G., Widmann, M., Zappa, G., Walton, D., Gutiérrez, J. M., Hagemann,  
523 S., Richter, I., Soares, P. M., Hall, A. and Mearns, L. O.: Towards process-informed bias  
524 correction of climate change simulations, *Nature Climate Change*, 7(11), 764–773,  
525 doi:10.1038/nclimate3418, 2017.

526 Nijse, F. J., Cox, P. M. and Williamson, M. S.: Emergent constraints on transient climate  
527 response (TCR) and Equilibrium Climate sensitivity (ECS) from historical warming in  
528 CMIP5 and CMIP6 models, *Earth System Dynamics*, 11(3), 737–750, doi:10.5194/esd-11-  
529 737-2020, 2020.

530 Perlwitz, J.: Tug of war on the Jet Stream, *Nature Climate Change*, 1(1), 29–31,  
531 doi:10.1038/nclimate1065, 2011.

- 532 Persad, G., Samset, B. H., Wilcox, L. J., Allen, R. J., Bollasina, M. A., Booth, B. B. B., Bonfils,  
533 C., Crocker, T., Joshi, M., Lund, M. T., Marvel, K., Merikanto, J., Nordling, K., Undorf,  
534 S., van Vuuren, D. P., Westervelt, D. M., and Zhao, A.: Rapidly evolving aerosol  
535 emissions are a dangerous omission from near-term climate risk assessments,  
536 *Environmental Research: Climate*, 2, 032001, <https://doi.org/10.1088/2752-5295/acd6af>,  
537 2023.
- 538 Pielke, R. and Ritchie, J.: Distorting the view of our climate future: The misuse and abuse of  
539 climate pathways and scenarios, *Energy Research & Social Science*, 72, 101890,  
540 [doi:10.1016/j.erss.2020.101890](https://doi.org/10.1016/j.erss.2020.101890), 2021.
- 541 Polvani, L. M., Waugh, D. W., Correa, G. J. and Son, S.-W.: Stratospheric ozone depletion: The  
542 main driver of twentieth-century atmospheric circulation changes in the Southern  
543 Hemisphere, *Journal of Climate*, 24(3), 795–812, [doi:10.1175/2010jcli3772.1](https://doi.org/10.1175/2010jcli3772.1), 2011.
- 544 Revell, L. E., Robertson, F., Douglas, H., Morgenstern, O. and Frame, D.: Influence of ozone  
545 forcing on 21st century Southern Hemisphere surface westerlies in CMIP6 models,  
546 *Geophysical Research Letters*, 49(6), [doi:10.1029/2022gl098252](https://doi.org/10.1029/2022gl098252), 2022.
- 547 Riahi, K., van Vuuren, D. P., Kriegler, E., Edmonds, J., O'Neill, B. C., Fujimori, S., Bauer, N.,  
548 Calvin, K., Dellink, R., Fricko, O., Lutz, W., Popp, A., Cuaresma, J. C., KC, S., Leimbach,  
549 M., Jiang, L., Kram, T., Rao, S., Emmerling, J., Ebi, K., Hasegawa, T., Havlik, P.,  
550 Humpenöder, F., Da Silva, L. A., Smith, S., Stehfest, E., Bosetti, V., Eom, J., Gernaat, D.,  
551 Masui, T., Rogelj, J., Strefler, J., Drouet, L., Krey, V., Luderer, G., Harmsen, M.,  
552 Takahashi, K., Baumstark, L., Doelman, J. C., Kainuma, M., Klimont, Z., Marangoni, G.,  
553 Lotze-Campen, H., Obersteiner, M., Tabeau, A. and Tavoni, M.: The shared  
554 socioeconomic pathways and their energy, land use, and greenhouse gas emissions  
555 implications: An overview, *Global Environmental Change*, 42, 153–168,  
556 [doi:10.1016/j.gloenvcha.2016.05.009](https://doi.org/10.1016/j.gloenvcha.2016.05.009), 2017.
- 557 Schmidt, D. F. and Grise, K. M.: The response of local precipitation and sea level pressure to  
558 Hadley cell expansion, *Geophysical Research Letters*, 44(20), [doi:10.1002/2017gl075380](https://doi.org/10.1002/2017gl075380),  
559 2017.
- 560 Schwalm, C. R., Glendon, S. and Duffy, P. B.: RCP8.5 tracks cumulative CO<sub>2</sub> emissions,  
561 *Proceedings of the National Academy of Sciences*, 117(33), 19656–19657,  
562 [doi:10.1073/pnas.2007117117](https://doi.org/10.1073/pnas.2007117117), 2020.
- 563 Sherwood, S. C., Webb, M. J., Annan, J. D., Armour, K. C., Forster, P. M., Hargreaves, J. C.,  
564 Hegerl, G., Klein, S. A., Marvel, K. D., Rohling, E. J., Watanabe, M., Andrews, T.,  
565 Braconnot, P., Bretherton, C. S., Foster, G. L., Hausfather, Z., von der Heydt, A. S., Knutti,  
566 R., Mauritsen, T., Norris, J. R., Proistosescu, C., Rugenstein, M., Schmidt, G. A.,  
567 Tokarska, K. B. and Zelinka, M. D.: An assessment of Earth's climate sensitivity using  
568 multiple lines of evidence, *Reviews of Geophysics*, 58(4), [doi:10.1029/2019rg000678](https://doi.org/10.1029/2019rg000678),  
569 2020.

- 570 Simpson, I. R., McKinnon, K. A., Davenport, F. V., Tingley, M., Lehner, F., Al Fahad, A., and  
571 Chen, D.: Emergent Constraints on the Large-Scale Atmospheric Circulation and Regional  
572 Hydroclimate: Do They Still Work in CMIP6 and How Much Can They Actually  
573 Constrain the Future?, *Journal of Climate*, 34, 6355–6377, <https://doi.org/10.1175/jcli-d-21-0055.1>, 2021.
- 575 Simpson, I. R. and Polvani, L. M.: Revisiting the relationship between jet position, forced  
576 response, and annular mode variability in the southern midlatitudes, *Geophysical Research  
577 Letters*, 43, 2896–2903, <https://doi.org/10.1002/2016gl067989>, 2016.
- 578 Solomon, S., Thompson, D. W., Portmann, R. W., Oltmans, S. J. and Thompson, A. M.: On the  
579 distribution and variability of ozone in the tropical upper troposphere: Implications for  
580 tropical deep convection and chemical-dynamical coupling, *Geophysical Research Letters*,  
581 32(23), doi:10.1029/2005gl024323, 2005.
- 582 Spinoni, J., Barbosa, P., Buchignani, E., Cassano, J., Cavazos, T., Christensen, J. H.,  
583 Christensen, O. B., Coppola, E., Evans, J., Geyer, B., Giorgi, F., Hadjinicolaou, P., Jacob,  
584 D., Katzfey, J., Koenigk, T., Laprise, R., Lennard, C. J., Kurnaz, M. L., Li, D., Llopart, M.,  
585 McCormick, N., Naumann, G., Nikulin, G., Ozturk, T., Panitz, H.-J., Porfirio da Rocha, R.,  
586 Rockel, B., Solman, S. A., Syktus, J., Tangang, F., Teichmann, C., Vautard, R., Vogt, J.  
587 V., Winger, K., Zittis, G. and Dosio, A.: Future global meteorological drought hot spots: A  
588 study based on Cordex Data, *Journal of Climate*, 33(9), 3635–3661, doi:10.1175/jcli-d-19-  
589 0084.1, 2020.
- 590 Srikrishnan, V., Guan, Y., Tol, R. S. and Keller, K.: Probabilistic projections of Baseline  
591 Twenty-first century CO<sub>2</sub> emissions using a simple calibrated integrated assessment  
592 model, *Climatic Change*, 170(3-4), doi:10.1007/s10584-021-03279-7, 2022.
- 593 Staten, P. W., Lu, J., Grise, K. M., Davis, S. M. and Birner, T.: Re-examining tropical expansion,  
594 *Nature Climate Change*, 8(9), 768–775, doi:10.1038/s41558-018-0246-2, 2018.
- 595 Tao, L., Hu, Y. and Liu, J.: Anthropogenic forcing on the Hadley circulation in CMIP5  
596 simulations, *Climate Dynamics*, 46(9-10), 3337–3350, doi:10.1007/s00382-015-2772-1,  
597 2016.
- 598 Tierney, J. E., Poulsen, C. J., Montañez, I. P., Bhattacharya, T., Feng, R., Ford, H. L., Hönlisch,  
599 B., Inglis, G. N., Petersen, S. V., Sagoo, N., Tabor, C. R., Thirumalai, K., Zhu, J., Burls, N.  
600 J., Foster, G. L., Goddérís, Y., Huber, B. T., Ivany, L. C., Kirtland Turner, S., Lunt, D. J.,  
601 McElwain, J. C., Mills, B. J., Otto-Bliesner, B. L., Ridgwell, A. and Zhang, Y. G.: Past  
602 climates inform our future, *Science*, 370(6517), doi:10.1126/science.aay3701, 2020.
- 603 van Vuuren, D., Tebaldi, C., O’Neill, B. C., ScenarioMIP SSC and workshop participants.:  
604 Pathway to next generation scenarios for CMIP7, doi:10.5281/zenodo.818611, 2023.

- 605 Watt-Meyer, O., Frierson, D. M. and Fu, Q.: Hemispheric asymmetry of tropical expansion  
606 under co2 forcing, *Geophysical Research Letters*, 46(15), 9231–9240,  
607 doi:10.1029/2019gl083695, 2019.
- 608 Waugh, D. W., Garfinkel, C. I. and Polvani, L. M.: Drivers of the recent tropical expansion in  
609 the Southern Hemisphere: Changing ssts or ozone depletion?, *Journal of Climate*, 28(16),  
610 6581–6586, doi:10.1175/jcli-d-15-0138.1, 2015.
- 611 World Meteorological Organization (WMO), *Scientific Assessment of Ozone Depletion: 2022*,  
612 GAW Report No. 278, 509 pp., WMO, Geneva, 2022.
- 613 Xia, Y., Hu, Y. and Liu, J.: Comparison of trends in the Hadley circulation between CMIP6 and  
614 CMIP5, *Science Bulletin*, 65(19), 1667–1674, doi:10.1016/j.scib.2020.06.011, 2020.
- 615 Xu, Z., Han, Y., Tam, C.-Y., Yang, Z.-L. and Fu, C.: Bias-corrected CMIP6 global dataset for  
616 dynamical downscaling of the historical and future climate (1979–2100), *Scientific Data*,  
617 8(1), doi:10.1038/s41597-021-01079-3, 2021.
- 618 Zhao, X., Allen, R. J., Wood, T., and Maycock, A. C.: Tropical Belt Width Proportionately More  
619 Sensitive to Aerosols Than Greenhouse Gases, *Geophysical Research Letters*, 47,  
620 <https://doi.org/10.1029/2019gl086425>, 2020.

621

622

## 623 **Acknowledgements**

624

625 The authors acknowledge the Climate Data Store for providing ERA5 data  
626 (<https://cds.climate.copernicus.eu>) as well as the CEDA archive for providing CMIP6 data  
627 (<https://catalogue.ceda.ac.uk>). We acknowledge the World Climate Research Programme,  
628 which, through its Working Group on Coupled Modeling, coordinated and promoted CMIP6. We  
629 thank the climate modeling groups for producing and making available their model output.

630

## 631 **Declarations**

## 632 **Funding**

633 This work has been funded by NSF Grant 2103013.

## 634 **Competing Interests**

635 The authors have no competing interests.

636 **Author Contributions**

637 DB performed the numerical analysis and wrote the initial draft of the manuscript. Both authors  
638 were equally involved in the design of the study, the interpretation of the results, and the review  
639 of the manuscript.

640 **Ethics Approval**

641 Not applicable

642 **Consent to Participate**

643 Not applicable

644 **Consent for Publication**

645 Not applicable

646 **Code and Data Availability**

647 CMIP6 data was acquired from the CEDA Archive <https://catalogue.ceda.ac.uk>. ERA5 data can  
648 be downloaded at <https://cds.climate.copernicus.eu> (Hersbach et al., 2020).

649

650

651

652

653

654

655

656

657

658

659

660

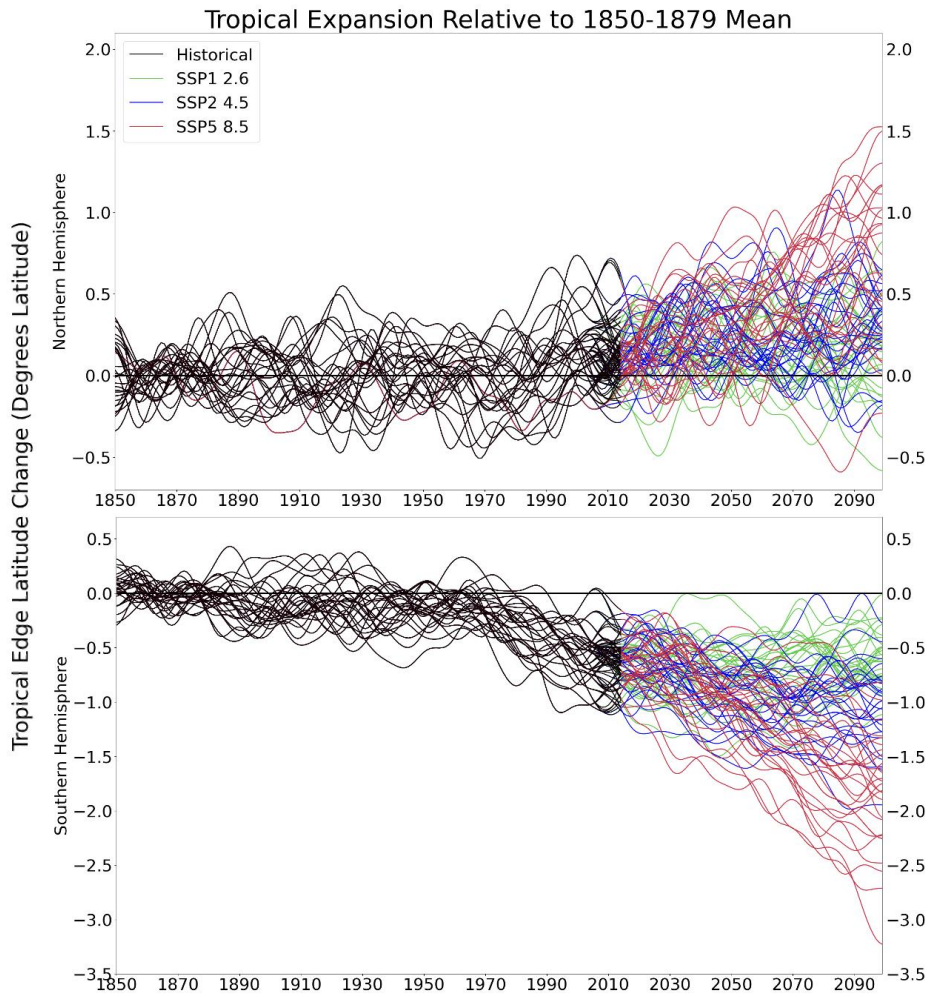
661 **Supplement**

662 **A Simple Framework for Likely Climate Projections Applied to Tropical Width**

663  
664 Text S1: Tropical edge latitude change for all simulations

665  
666 Tropical edge latitude change for all models using all forcing levels. In the NH the intermodel  
667 differences are larger than the inter-forcing differences. In the SH the inter-forcing differences are  
668 greater than the intermodel differences. Overall, the intermodel spread is similar in both  
669 hemispheres, so this difference is a result of hemispheric differences in sensitivity.

670



671  
672  
673 Fig. S1: Tropical edge latitude change for all simulations grouped by forcing level (color) in both  
674 hemispheres. All changes are relative to the 1850-1879 mean.

675  
676  
677  
678



679 Text S2: Annotated tropical expansion by historical tropical width showing debiasing methods

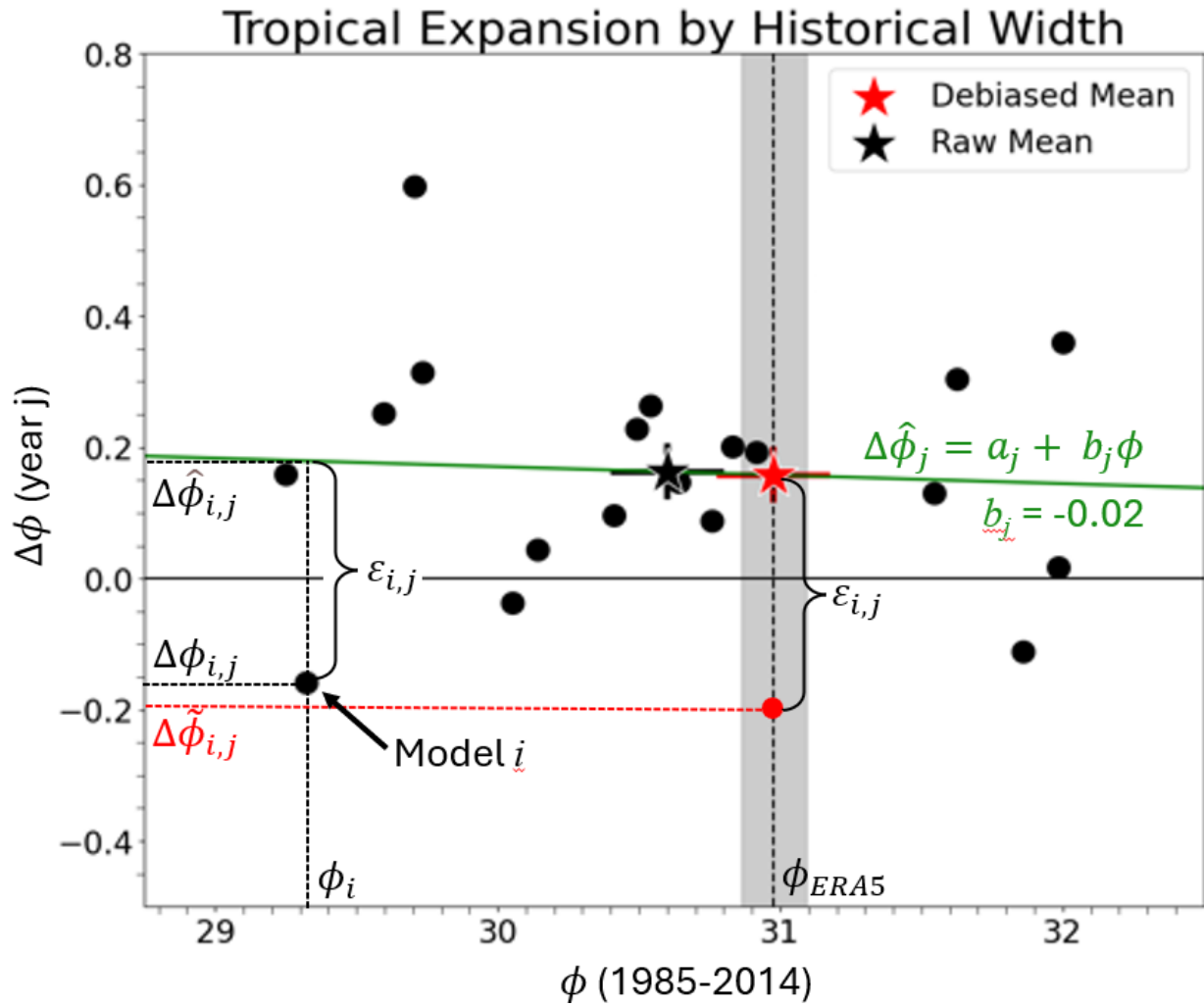
680

681 Tropical expansion in year  $j$  (2084) by 1985-2014 tropical width in the Southern Hemisphere

682 showing variables and methods included in the debiasing for an individual model  $i$ . The debiasing

683 results in a slight increase in projected expansion for this model.

684



685

686

687 Fig. S2: Tropical widening in 2070-2099 relative to 1985-2014 by tropical width in 1985-2014 for

688 SSP2-4.5 models with likely TCR. The debiasing is demonstrated for a single model.